ISSN 1573-160X, *PHYSICAL OCEANOGRAPHY*, Vol. 31, Iss. 2, pp. 284-294 (2024)

published in *Morskoy Gidrofizicheskiy Zhurnal*, 2024, Vol. 40, Iss. 2, pp. 312–324

Original article

Evaluation of Sea Ice Drift in the Arctic Marginal Ice Zone based on Sentinel-1A/B Satellite Radar Measurements

E. V. Plotnikov [1, ✉], **I. E. Kozlov** [1], **E. V. Zhuk** [1], **A. V. Marchenko** [2]

[1] *Marine Hydrophysical Institute of RAS, Sevastopol, Russian Federation*
[2] *University Centre in Svalbard, Longyearbyen, Norway*
✉ *ev.plotnikov@ya.ru*

Abstract

Purpose. The object of the work is to construct an automated system for calculating sea ice drift velocity fields using Sentinel-1A/B radar measurements based on the normalized maximum cross-correlation approach. The conditions and results of a numerical experiment aimed at evaluating the effectiveness of this technique for 63 pairs of radar images of the Fram Strait region for the summer-autumn periods in 2017 and 2018 are presented. Both the calculation algorithm and the qualitative and quantitative characteristics of the results are described in details. The effectiveness of the approach being applied to regular monitoring of ice drift is considered.

Methods and Results. The maximum cross-correlation (MCC) approach was used for calculations. It is based on automated finding of photographically similar fragments in the pairs of images with a known sensing time interval. The Pearson correlation coefficient was applied as a proximity metric. As a result, 63 sea ice drift velocity fields were constructed in the Fram Strait region, each with a spatial scale of approximately several hundred thousand square kilometers. The method for filtering false correlations is proposed.

Conclusions. The approach applied in the study makes it possible to obtain automatically the sea ice drift velocity fields from the satellite data with high spatial resolution (40 m). The reconstructed velocity fields cover significant areas of the ocean surface. The method proposed for filtering false correlations permits to extract effectively the fragments with distortions resulting from the MCC algorithm limitations, from the calculation results.

Keywords: sea ice drift dynamics, sea ice, optical flow, maximum cross-correlation approach, Sentinel-1A/B images, Fram Strait, Arctic Ocean

Acknowledgements: The study was carried out with financial support of the Russian Science Foundation grant No. 21–17–00278 (analysis, validation and development of a web-service to store sea ice drift fields) and within the framework of the theme of state assignment № FNNN-2024-0017 (development of the method for calculating sea ice drift velocity based on satellite radar data).

For citation: Plotnikov, E.V., Kozlov, I.E., Zhuk, E.V. and Marchenko, A.V., 2024. Evaluation of Sea Ice Drift in the Arctic Marginal Ice Zone Based on Sentinel-1A/B Satellite Radar Measurements. *Physical Oceanography*, 31(2), pp. 284-294.

Introduction

Sea ice drift monitoring is an important component of the Arctic geophysical process research. The data obtained can be used to solve a wide range of theoretical and practical problems. Nowadays, one of the most promising approaches to solve this problem is the analysis of satellite images in visible, infrared and microwave ranges. Sequences of satellite images related to the same fragment of the sea surface and a narrow time interval can be used to simulate sea surface dynamics, in particular, sea ice drift velocity and direction. At the same time, approaches for calculating optical flow are often used to solve the problem described. Extensive

literature on this approach describes both algorithms and features of their use in practice depending on the source data specifics [1–9]. The calculation automation problem is relevant due to the volume of satellite image archives available today. Its successful solution opens up the possibility of obtaining regular and long-term observations of sea ice drift dynamics.

This direction has received widespread development in the last decade; the research results are presented, e.g., in [10–14]. In this case, various tracking algorithms are used in relation to the data from MODIS, Sentinel-1, Sentinel-2, Landsat-8 and a number of others, mainly in the optical range. Important factors are source image resolution, ability to effectively optimize calculations for processing large amounts of data and automation of calculations. The present paper describes an automated approach making it possible to estimate sea ice dynamics from radar images with a resolution of 40 m covering an area of approximately several hundred thousand square kilometers. According to the authors, practical results on the use of an automatic data processing system with such parameters are published for the first time.

After the launch of Sentinel-1A/B synthetic aperture radar (SAR) satellites, obtaining pairs of radar images of the Arctic Region with a short time delay became possible, which offered an opportunity to evaluate the kinematic characteristics of various meso- and submesoscale processes in the upper layer of the Arctic seas [15–19]. In the application to the evaluation of ice drift velocity fields in [16], the authors demonstrated the possibility of effective calculation of such fields in the areas of intense eddy dynamics in the marginal ice zone (MIZ) with a spatial resolution O(100 m) based on the maximum cross-correlation approach. In [20, 21], the authors applied machine-learning methods to identify the MIZ eddies in satellite SAR data in order to show further development of this direction.

The present paper aims at describing general methodology and demonstrating effectiveness of the computational scheme for automatic Sentinel–1A/B satellite data processing to simulate sea ice drift fields in the MIZ. The proposed methodology was applied to a three-month data set related to the Fram Strait region. The approach used made it possible to automatically process a statistically significant amount of data and obtain high-quality results that confirm the approach effectiveness for quick monitoring of ice field drift dynamics in the marginal ice zone of the Arctic.

Data and methods

Sentinel-1A/B radar images obtained for the Fram Strait region in 2017 and 2018 represented initial data. Specifically, L1 Ground Range Detected products with a 40 × 40 m pixel and a spatial resolution of 93 × 87 m in Extra Wide Swath shooting mode were used. Satellite radar images were obtained from the archives of the Copernicus Open Access Hub service (https://scihub.copernicus.eu).

A total of 63 pairs of images obtained in September 2017, as well as in July and September 2018, were selected. The time range between successive measurements was from 48 to 52 minutes for each pair of radar images, which were chosen based on considerations of information content determined by the manifestation of surface structures in the drifting ice field. The data were interpolated onto a regular grid with 40 × 40 m resolution and then the intersections of the scanned areas were identified

on each radar image. Additionally, the images were smoothed using a median filter with a sliding window of 20 × 20 pixels. Fig. 1 shows a pair of Sentinel-1A/B radar images for 26 July 2018 obtained in this way.

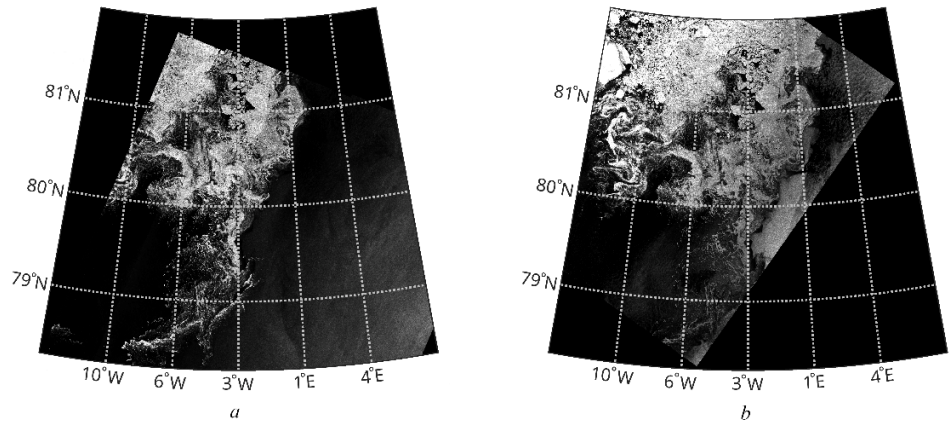

F i g. 1. A pair of Sentinel-1A (a) and Sentinel-1B (b) radar images for 15 September 2018 with the drifting ice present in the marginal ice zone of the Fram Strait

The main algorithm used in data processing is provided by the normalized maximum cross-correlation (MCC) approach [1, 3, 4, 6, 7, 9] based on obtaining the most correlated fragments in the analyzed images, the displacement of which from each other does not exceed the theoretically possible one. The neighborhoods of each pixel in both images are selected and then a normalized cross-correlation function is constructed for them. The deviation of this function maximum position from the central point is taken as the desired shift, i.e., the displacement of a texture fragment from image to image. Formally, the approach can be described as follows: the image matrices are denoted as I_1 and I_2. Let us consider a pixel with *i* and *j* indices. Let the neighborhood have a square shape and size $N \times N$, where N is odd;

$$k = \left\{ i - (N-1)/\frac{2}{i} + (N-1)/2, \quad l = \left\{ j - (N-1)/\frac{2}{j} + (N-1)/2 \right\} \right\},$$

$$M_1 = \frac{1}{N^2} \sum_{k,1} I_1(k,l) \text{ and } M_2(u,v) = \frac{1}{N^2} \sum_{k,1} I_2(k+u, l+v).$$

Then the normalized cross-correlation function will have the following form:

$$F(u,v,i,j) = \frac{\sum_{i,k} \left(I_1(k,l) - M_1 \right) \left(I_2(k+u, l+v) - M_2(u,v) \right)}{\sqrt{\left(\sum_{l,k} \left(I_1(k,l) - M_1 \right)^2 \right) \left(\sum_{l,k} \left(I_2(k+u, l+v) - M_2 \right)^2 \right)}}.$$

Here $-u_{\max} \le u \le u_{\max}$, $-v_{\max} \le v \le v_{\max}$, where $u_{\max}$ and $v_{\max}$ are specified maximum possible shifts in both coordinates. The required values u_0 and v_0 for the pixel with i and j indices are such that $F\left((u_0, v_0, i, j) = \max\left(F(u, v, i, j)\right)\right)$, where u and v take values from the interval above. After finding the described values for all $(N-1)/2 < i < S_1 - (N-1)/2 + 1$ and $(N-1)/2 < j < -(N-1)/2 + 1$, where (S_1, S_2) is size of the images, we obtain U and V matrices of size $(S_1 - N - u_{\max} + l, S_2 - N - v_{\max} + l)$.

Figure 2 shows both components (u_0 and v_0) of the vector field constructed in this way with parameters $N = 80$ $u_{\max} = v_{\max} = 50$ according to the data shown in Fig. 1.

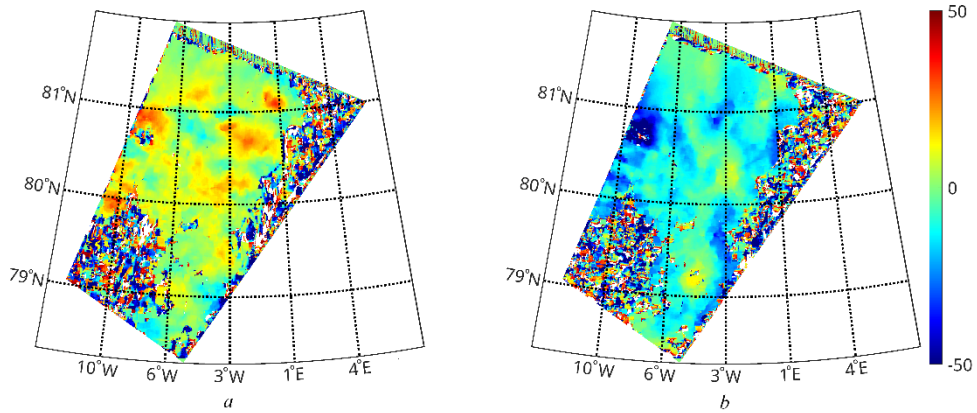

F i g. 2. Pixel shifts corresponding to the velocity field components u_0 (*a*) and v_0 (*b*) and obtained on 26 July 2018 using the MCC algorithm for the Sentinel-1A/B radar images

The correspondence of the fragments containing useful data to the fragments where the presence of ice accumulations in the original images is clearly visible is noteworthy here. The rest of the image is either uninformative or contains noise, which is a manifestation of an effect called “spurious correlations.” The principal generally accepted approach for filtering corresponding fragments is a lower limit for the minimum value of the cross-correlation function and cutting off pixels that do not satisfy this condition. Obviously, a morphological analysis of the resulting field could be an effective approach here. However, the authors decided to take a different path taking into account that operator $(I_1, I_2) \to (U, V)$ is not symmetric.

Let us denote the indices of its neighborhood as $k = \left\{ i - (N-1)/\frac{2}{i} + (N-1)/2 \right\}$, $l = \left\{ j - (N-1)/\frac{2}{j} + (N-1)/2 \right\}$. Suppose (u_0, v_0) is the calculated shift and for any displacements fragment $I_1(k, l)$ is maximally correlated with fragment $I_2(k + u_0, l + v_0)$. Then correlation of $I_1(k - u_0, l + v_0)$ and $I_2(k, l)$ should also be high. Therefore, if the described

calculation is carried out taking I_2 as the first image and I_1 as the second one, the results should be close when the signs of both components change. Let us name this as an inverse calculation. The cosine of the angle between the vectors of two such fields can be used to estimate proximity. Figure 3, *a* shows the values of this quantity. Here, the correspondence of fragments with high cosine values to fragments with informative data is clearly visible, which confirms the effectiveness of the approach described. It is possible to obtain a mask for which the calculated velocity fields are relevant by setting the optimal threshold value. A threshold of 0.92 was used for calculations. In addition, a gradient filter can be used to highlight high spatial heterogeneity areas in order to remove residual noise. The maximum value of the variation of the *u* and *v* components in a neighborhood of 3 × 3 pixels (Fig. 3, *b*) is chosen for each pixel. All fragments exceeding a threshold value of 2.51 are cut off.

After implementing the described filtering procedure, a number of small individual fragments with doubtful information content remain in the resulting mask. To remove them, the mask is divided into connected components and the number of pixels contained is calculated for each of them. The component is cut if this number is less than the specified threshold. The component area ratio to the area of the entire scene was chosen as the evaluation value and the value of 0.25% was chosen as the threshold.

To summarize all the aforesaid, we can briefly describe the algorithm for processing a pair of radar images as follows:

– unpacking and reprojection of source data onto a regular grid;

– direct and inverse calculations using the normalized maximum cross-correlation approach;

– filtering of irrelevant fragments;

– compression of the scene taking into account the boundaries of the mask obtained at the previous step;

– removal of small individual mask components;

– transformation of shifts into a velocity (m/s) field.

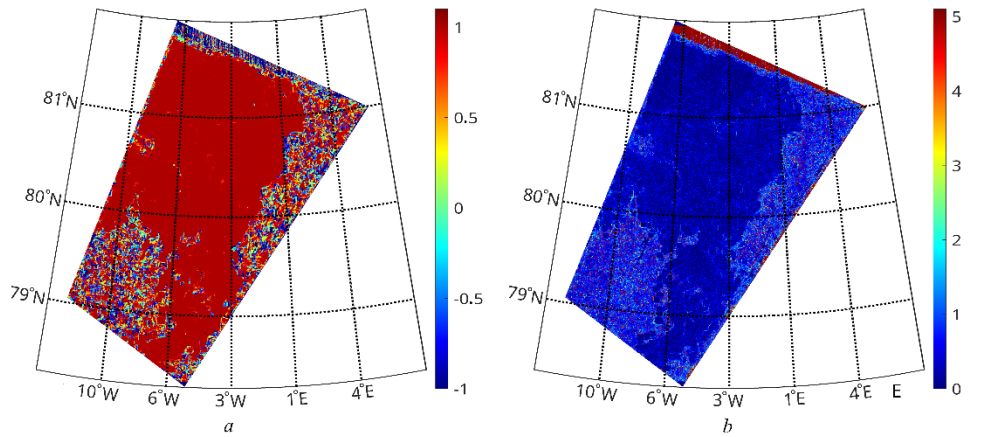

F i g. 3. Spatial distribution of the cosine of angle between the vectors of calculated shifts resulted from direct and inverse calculations (*a*); assessment of the homogeneity of the shift components over the 3 × 3 pixel window (*b*)

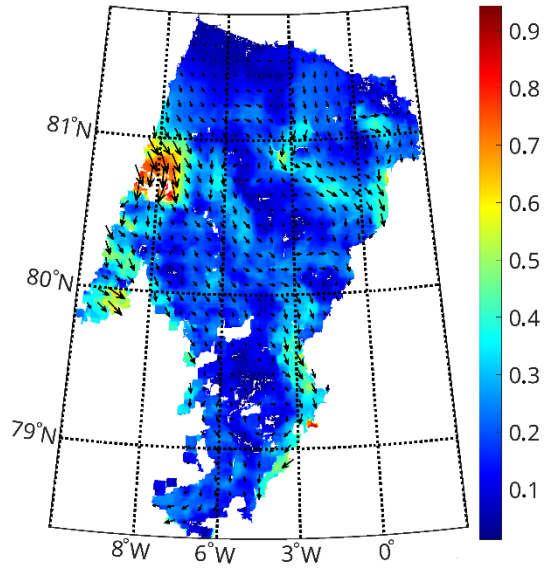

Fig. 4. Final result of calculation of the ice drift velocity (m/s) field in the Fram Strait for 26 July 2018

The entire data processing result is shown in Fig. 4. It can be seen that the range of observed ice drift velocities is 0.1–0.8 m/s, the average speed is ~ 0.2–0.3 m/s, the dominant direction of ice drift is southern/southeastern. Maximum drift speeds are observed in the northwestern sector, as well as on the southeastern periphery of the area shown.

Results

The results of calculations are 63 vector fields of ice drift velocity describing the horizontal movement of sea ice accumulations in the Fram Strait MIZ. For a pair of images (10,000 × 10,000 pixels), the running time of the used implementation of the MCC algorithm with a sliding window size of 80×80 and maximum shifts $u_{\max} = 50, v_{\max} = 50$ is about two hours, when calculated in two threads on a computer with Intel i5 12500H processor running Debian GNU/Linux 12 operating system.

An objective evaluation of the described approach effectiveness is difficult due to the lack of reference data on surface sea dynamics. The most promising approach in the present case seems to be a comparison of the velocity fields modelled from satellite data with field data on the direction and speed of the ice drift obtained based on the stationary geolocation sensors (GPS trackers) installed on ice floes. Figure 5 shows the drift trajectory of such a sensor against the velocity field background calculated from satellite data.

Unfortunately, the authors do not have a statistically significant array of field data for a more detailed comparison. However, Fig. 5 shows that measurements from two independent sources agree well in direction and absolute value. In addition, a certain idea of the approach relevance can be obtained based on the expert evaluation of the structure of the modelled fields and the correspondence of the visible displacements of contrast structures in image textures to the calculated

shifts. From this viewpoint, the calculation results demonstrate high quality. Fragments with clearly visible inconsistencies are effectively eliminated using an automatic filtering procedure while the number of discarded pixels is negligible compared to their total number in areas with well-defined contrasts. This algorithm demonstrated no significant redundancy or insufficiency. Mesoscale and submesoscale dynamic structures (such as individual eddies, eddy dipoles or ice filaments) visible in the images are also clearly seen in the velocity fields obtained.

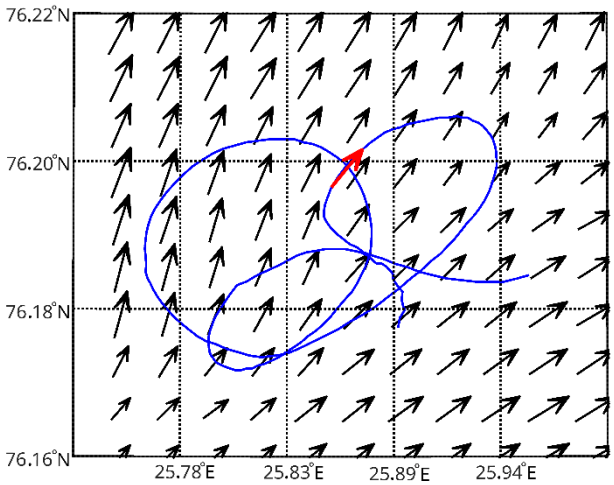

F i g. 5. Comparison of the ice drift velocity vectors derived from satellite data with the field measurements obtained from the data of GPS trackers installed on ice. Blue curve shows the trajectory of ice floes based on the field data. Red arrow highlights a fragment of field measurements coinciding in time with satellite imagery. Time of Sentinel-1 acquisitions: at 5:02 UTC and at 5:51 UTC on 26.04.2019. GPS tracker is traced from 26.04.2019 (00:10) to 27.04.2019 (11:30)

Visualization of satellite products with ice drift fields

At the next stage, the products with sea ice drift velocity fields simulated from quasisynchronous satellite data are posted on the webpage of Laboratory of Marine Polar Research (LMPR) of Marine Hydrophysical Institute of RAS at http://polar-space.ru/arctic_currents. To do this, the calculated fields are first interpolated onto a grid with a 40 m step and recorded as netCDF files. A data visualization system based on client-server architecture was developed for the Web. Figure 6 shows the general structure of the visualization system for this satellite product.

This system stores netCDF format data with ice drift fields as a file archive on the server. A special software module was developed in Python to display ice drift velocities on a geographic map. It converts the source data into images with a single speed scale for all files. The name of each picture file contains a date in order to establish a one-to-one correspondence between a user request and a displayed ice drift field.

The user interface (UI) for selecting and displaying the product of interest was developed using jQuery javascript libraries. The map service functions are implemented using the mapBox GL library. The UI makes it possible to select the ice drift field for the date of interest by scrolling through an array of dates or selecting the desired date from the list. Figure 7 shows an example of the UI at http://polar-space.ru/arctic currents for the selected date 26 July 2018.

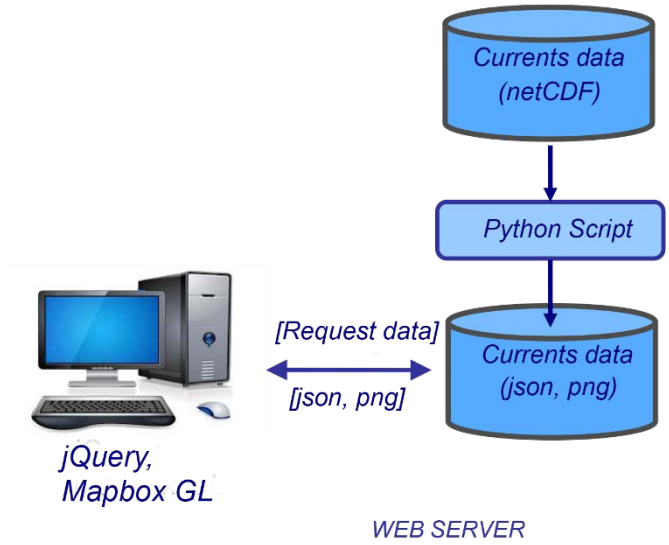

F i g. 6. General structure of the system for visualizing the products with ice drift fields (available at http://polar-space.ru/arctic_currents)

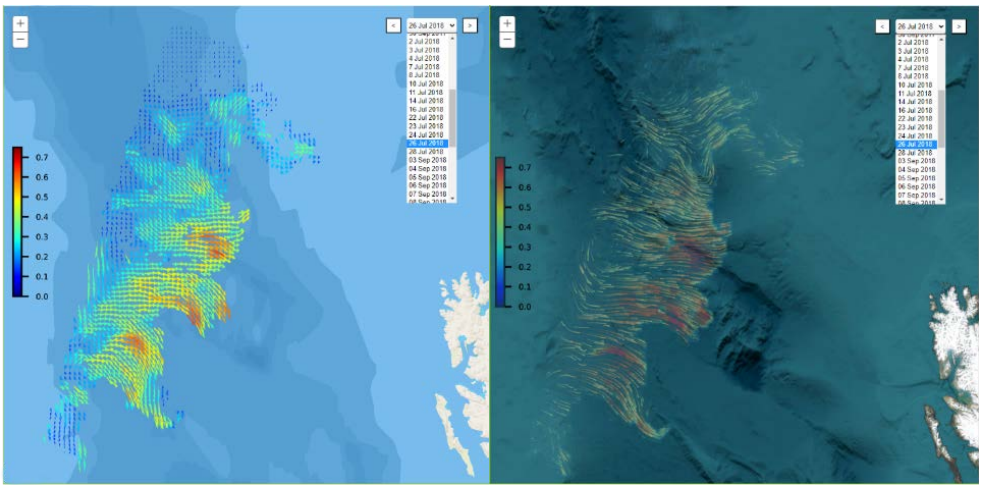

F i g. 7. User interface of the system for visualizing the products with ice drift fields in the marginal ice zone of the Fram Strait for 26 July 2018. *On the left* is an example of a static display of ice drift fields, *on the right* – a dynamic field using the Wind-JS library

The developed UI contains a choice of displaying data with ice drift fields in the form of not only a static picture (Fig. 7, left), but also a dynamic field (Fig. 7, right). This task is implemented with the Wind-JS library (https://github.com/Esri/wind-js) adapted to display ice drift vectors. The input data are json files containing the values of the ice drift zonal and meridional components. A special software module was developed in Python to generate these files automatically. To date, all processed data for 2017 and 2018 have been posted on the LMPR MHI website. In addition, the existing interface is supplemented with the ability to download ice drift fields of interest in netCDF format.

Conclusion

The paper describes the general methodology for processing quasisynchronous measurements of Sentinel–1A/B satellite SARs operating in tandem for 5 years (2016–2021) to obtain time-regular ice drift velocity fields in the Arctic marginal ice zone. As a rule, temporal resolution of the resulting products with ice drift velocity fields is 1 day in the European sector of the Arctic and from 1 to 5 days in other Arctic regions.

Limited to the initial data set, validation of the resulting velocity fields with *in situ* measurements showed good agreement between them. Nevertheless, the research will be continued in this direction to determine objective statistics of the quality of calculated ice drift velocity fields.

Compared to the existing products concerning ice drift in the Arctic, the presented approach and the simulated velocity fields are distinguished by a significantly higher spatial resolution (40 m), relative simplicity of the methods used and low requirements for computing resources.

The resulting products with ice drift velocity fields in the marginal ice zone of the Arctic are available at http://polar-space.ru/arctic currents and can be used by specialists to solve a number of practical problems including evaluation of the MIZ dynamics and evolution and processes in it, as well as for comparison with other satellite products and validation of ocean general circulation models with lower resolution.

Sentinel–1A/B data were obtained from the archives of the Copernicus Open Access Hub service (available at: https://scihub.copernicus.eu).

REFERENCES

1. Alexanin, A.I., Alexanina, M.G. and Karnatsky, A.Y., 2013. Automatic Computation of Sea Surface Velocities on a Sequence of Satellite Images. *Current Problems in Remote Sensing of the Earth from Space*, 10(2), pp. 131-142 (in Russian).

2. Beauchemin, S.S. and Barron, J.L., 1995. The Computation of Optical Flow. *ACM Computing Surveys (CSUR)*, 27(3), pp. 433-466. https://doi.org/10.1145/212094.212141

3. Barron, J.L. and Thacker, N.A., 2005. *Tutorial: Computing 2D and 3D Optical Flow*. Imaging Science and Biomedical Engineering Division, Medical School, University of Manchester. Vol. 1. https://faculty.runi.ac.il/toky/old_courses/videoproc-07/handouts/2004-012.pdf [Accessed: 10 April 2024].

4. Emery, W.J., Thomas, A.C., Collins, M.J., Crawford, W.R. and Mackas, D.L, 1986. An Objective Method for Computing Advective Surface Velocities from Sequential Infrared Satellite Images. *Journal of Geophysical Research: Oceans*, 91(C11), pp. 12865-12878. https://doi.org/10.1029/JC091iC11p12865

5. Fortun, D., Bouthemy, P. and Kervrann, C., 2015. Optical Flow Modeling and Computation: A Survey. *Computer Vision and Image Understanding*, 134, pp. 1-21. https://doi.org/10.1016/j.cviu.2015.02.008

6. Luo, J. and Konofagou, E., 2010. A Fast Normalized Cross-Correlation Calculation Method for Motion Estimation. *IEEE Transactions on Ultrasonics, Ferroelectrics, and Frequency Control*, 57(6), pp. 1347-1357. https://doi.org/10.1109/TUFFC.2010.1554

7. Lawrence, P., 2016. The Derivation of Sea Surface Velocities from Satellite Imagery Using Maximum Cross Correlation (MCC). The *Plymouth Student Scientist*, 9(1), pp. 145-161. http://hdl.handle.net/10026.1/14119

8. Stark, M., 2013. *Optical Flow PIV: Improving the Accuracy and Applicability of Particle Image Velocimetry*. MS Thesis. ETH. Department of Mechanical and Process Engineering. https://doi.org/10.3929/ethz-a-009767070

9. Sun, D., Roth, S., Lewis, J.P. and Black, M.J., 2008. Learning Optical Flow. In: D. Forsyth, P. Torr, A. Zisserman, eds., 2008. *Computer Vision–ECCV 2008*. *ECCV 2008*. Lecture Notes in Computer Science, vol. 5304. Springer, Berlin, Heidelberg, pp. 83-97. https://doi.org/10.1007/978-3-540-88690-7_7

10. Kwok, R., Schweiger. A., Rothrock, D.A., Pang, S. and Kottmeier, C., 1998. Sea Ice Motion from Satellite Passive Microwave Imagery Assessed with ERS SAR and Buoy Motions. *Journal of Geophysical Research: Oceans*, 103(C4), pp. 8191-8214. https://doi.org/10.1029/97JC03334

11. Samardžija, I., 2018. Two Applications of a Cross-Correlation Based Ice Drift Tracking Algorithm; Ship-Based Marine Radar Images and Camera Images from a Fixed Structure. In: FEDU, 2018. *Proceedings of the 24th IAHR International Symposium on Ice*. Vladivostok: Far Eastern Federal University, pp. 141-151.

12. Lopez-Acosta, R., Schodlok, M.P. and Wilhelmus, M.M., 2019. Ice Floe Tracker: An Algorithm to Automatically Retrieve Lagrangian Trajectories via Feature Matching from Moderate-Resolution Visual Imagery. *Remote Sensing of Environment*, 234, 111406. https://doi.org/10.1016/j.rse.2019.111406

13. Wang, M., König, M. and Oppelt, N., 2021. Partial Shape Recognition for Sea Ice Motion Retrieval in the Marginal Ice Zone from Sentinel-1 and Sentinel-2. *Remote Sensing*, 13(21), 4473. https://doi.org/10.3390/rs13214473

14. Howell, S.E.L., Brady, M. and Komarov, A.S., 2022. Generating Large-Scale Sea Ice Motion from Sentinel-1 and the RADARSAT Constellation Mission Using the Environment and Climate Change Canada Automated Sea Ice Tracking System. The *Cryosphere*, 16(3), pp. 1125-1139. https://doi.org/10.5194/tc-16-1125-2022

15. Kozlov, I.E. and Mikhaylichenko, T.V., 2021. Estimation of Internal Wave Phase Speed in the Arctic Ocean from Sequential Spaceborne SAR Observations. *Current Problems in Remote Sensing of the Earth from Space*, 18(5), pp. 181-192. https://doi.org/10.21046/2070-7401-2021-18-5-181-192 (in Russian).

16. Kozlov, I.E., Plotnikov, E.V. and Manucharyan, G.E., 2020. Brief Communication: Mesoscale and Submesoscale Dynamics in the Marginal Ice Zone from Sequential Synthetic Aperture Radar Observations. *The Cryosphere*, 14(9), pp. 2941-2947. https://doi.org/10.5194/tc-14-2941-2020

17. Kozlov, I.E. and Atadzhanova, O.A., 2021. Eddies in the Marginal Ice Zone of Fram Strait and Svalbard from Spaceborne SAR Observations in Winter. *Remote Sensing*, 14(1), 134. https://doi.org/10.3390/rs14010134

18. Artamonova, A.V. and Kozlov, I.E., 2023. Eddies in the Norwegian and Greenland Seas from the Spaceborne SAR Observations in Summer, 2007. *Physical Oceanography*, 30(1), pp. 112-123. https://doi.org/10.29039/1573-160X-2023-1-112-123

19. Marchenko, A.V., Morozov, E.G., Kozlov, I.E. and Frey, D.I., 2021. High-Amplitude Internal Waves Southeast of Spitsbergen. *Continental Shelf Research*, 227, 104523. https://doi.org/10.1016/j.csr.2021.104523

20. Khachatrian, E. and Sandalyuk, N., 2022. On the Exploitation of Multimodal Remote Sensing Data Combination for Mesoscale/Submesoscale Eddy Detection in the Marginal Ice Zone. *IEEE Geoscience and Remote Sensing Letters*, 19, pp. 1-5. https://doi.org/10.1109/LGRS.2022.3215202

21. Khachatrian, E., Sandalyuk, N. and Lozou, P., 2023. Eddy Detection in the Marginal Ice Zone with Sentinel-1 Data Using YOLOv5. *Remote Sensing*, 15(9), 2244. https://doi.org/10.3390/rs15092244

Submitted 06.09.2023; approved after review 29.12.2023;
accepted for publication 18.01.2024.

About the authors:

Evgeniy V. Plotnikov, Junior Researcher, Marine Hydrophysical Institute of RAS (2 Kapitanskaya Str., Sevastopol, 299011, Russian Federation), **ORCID ID: 0000-0003-4365-9369**, **Scopus Author ID: 57190382092**, **SciProfiles: 2325823**, ev.plotnikov@ya.ru

Igor E. Kozlov, Leading Researcher, Head of Marine Polar Research Laboratory, Marine Hydrophysical Institute of RAS (2 Kapitanskaya Str., Sevastopol, 299011, Russian Federation), CSc. (Phys.-Math.), **ORCID ID: 0000-0001-6378-8956**, **ResearcherID: G-1103-2014**, **Scopus Author ID: 49963767500**, ik@mhi-ras.ru

Elena V. Zhuk, Junior Researcher, Marine Hydrophysical Institute of RAS (2 Kapitanskaya Str., Sevastopol, 299011, Russian Federation), **ORCID ID: 0000-0002-4263-7734**, **Scopus Author ID: 57191412660**, alenixx@gmail.com

Aleksey V. Marchenko, Department of Arctic Technologies, University Centre in Svalbard (P.O. Box 156 N-9171 Longyearbyen, Norway), CSc. (Phys.-Math.), Professor, **ORCID ID: 0000-0003-4169-0063**, **Scopus Author ID: 7101880290, ResearcherID: GSD-3516-2022**, aleksey.marchenko@unis.no

Contribution of the co-authors:

Evgeniy V. Plotnikov – methodology and software development, carrying out numerical experiments, preparation of the article text

Igor E. Kozlov – problem statement, data and article text preparation

Elena V. Zhuk – development of the data access web resource, web database formation, preparation of the article text

Aleksey V. Marchenko – preparation of GPS tracker data

The authors have read and approved the final manuscript.
The authors declare that they have no conflict of interest.